ISSN 1674-1056
http://cpb.iphy.ac.cn
http://iopscience.iop.org/cpb
中国物理 B
Chinese Physics
中国物理 Chinese Physics B

Subwavelength asymmetric Au-VO_2 nanodisk dimer for switchable directional scattering

Han-Mou Zhang(张汉谋), Wu-Yun Shang(尚武云), Hua Lu(陆华), Fa-Jun Xiao(肖发俊), Jian-Lin Zhao(赵建林)

Citation: Chin. Phys. B . 2018, 27(11): 117301. **doi:** 10.1088/1674-1056/27/11/117301

Journal homepage: http://cpb.iphy.ac.cn; http://iopscience.iop.org/cpb

What follows is a list of articles you may be interested in

Selective enhancement of green upconversion luminescence of Er-Yb: $NaYF_4$ by surface plasmon resonance of $W_{18}O_{49}$ nanoflowers and applications in temperature sensing

Ang Li(李昂), Jin-Lei Wu(吴金磊), Xue-Song Xu(许雪松), Yang Liu(刘洋), Ya-Nan Bao(包亚男), Bin Dong(董斌)
Chin. Phys. B . 2018, 27(9): 097301. **doi:** 10.1088/1674-1056/27/9/097301

Optical interaction between one-dimensional fiber photonic crystal microcavity and gold nanorod

Yang Yu(于洋), Ting-Hui Xiao(肖廷辉), Zhi-Yuan Li(李志远)
Chin. Phys. B . 2018, 27(1): 017301. **doi:** 10.1088/1674-1056/27/1/017301

Tunable multiple plasmon resonances and local field enhancement of nanocrescent/nanoring structure

Wang Bin-Bing, Zhou Jun, Chen Dong, Fang Yun-Tuan, Chen Ming-Yang
Chin. Phys. B . 2015, 24(8): 087301. **doi:** 10.1088/1674-1056/24/8/087301

Deep-ultraviolet surface plasmon resonance of Al and Al_{core}/Al_2O_{3shell} nanosphere dimers for surface-enhanced spectroscopy

Ci Xue-Ting, Wu Bo-Tao, Song Min, Chen Geng-Xu, Liu Yan, Wu E, Zeng He-Ping
Chin. Phys. B . 2014, 23(9): 097303. **doi:** 10.1088/1674-1056/23/9/097303

Fano-like resonance characteristics of asymmetric Fe_2O_3@Au core/shell nanorice dimer

Wang Bin-Bing, Zhou Jun, Zhang Hao-Peng, Chen Jin-Ping
Chin. Phys. B . 2014, 23(8): 087303. **doi:** 10.1088/1674-1056/23/8/087303

SPECIAL TOPIC — 80th Anniversary of Northwestern Polytechnical University (NPU)

Subwavelength asymmetric Au–VO_2 nanodisk dimer for switchable directional scattering*

Han-Mou Zhang(张汉谋), Wu-Yun Shang(尚武云), Hua Lu(陆华), Fa-Jun Xiao(肖发俊)†, and Jian-Lin Zhao(赵建林)‡

MOE Key Laboratory of Material Physics and Chemistry under Extraordinary Conditions, and Shaanxi Key Laboratory of Optical Information Technology, School of Science, Northwestern Polytechnical University, Xi'an 710129, China

(Received 14 July 2018; revised manuscript received 7 September 2018; published online 8 October 2018)

We propose an asymmetric Au–VO_2 nanodisk dimer for realizing a switchable directional scattering. Specifically, the directional scattering can be triggered on/off through controlling the phase transition of the VO_2 nanodisk from metallic to semiconductor state. More strikingly, an obvious directional scattering with the directivity of ~ 40 dB is achieved under the metallic state of VO_2 nanodisk. This tunable directional scattering is further explained with an interference model where the Au and VO_2 nanodisks are treated as two weakly interacting electric dipoles. The phase transition controlled scattering patterns of asymmetric Au–VO_2 nanodisk dimer are then well interpreted from the phase difference between these two dipoles.

Keywords: localized surface plasmon resonance, directional scattering, vanadium dioxide

PACS: 73.20.Mf, 42.70.–a, 42.25.Fx, 78.67.–n **DOI:** 10.1088/1674-1056/27/11/117301

1. Introduction

Metallic nanoparticles possess a lot of intriguing optical properties due to the localized surface plasmon resonances (LSPR) they support.[1] They show remarkable ability to confine light at nanoscale,[2–4] leading to giant enhancement of electromagnetic field,[5,6] which makes incredibly weak physics processes observable. This can be exemplified by the enhanced optical processes, including second harmonic generation (SHG),[7–10] multiphoton luminescence,[11] and surface-enhanced Raman scattering.[12] When two or more nanoparticles are placed together, a new set of hybridized collective plasmonic modes[13,14] can be observed due to their near field coupling. As a result, molding metallic nanoparticles to control their interactions can offer an effective approach to tailoring the field distribution in near field,[15] and also the spectral lineshape[16,17] and the scattering pattern in the far-field.[18,19] Shaping the scattering pattern, especially to achieve the directional scattering, is of significance to many fields such as nanoantennas, sensors, and photovoltaic devices.[18,20,21] As most materials have only dominant electric responses, conventional approaches to shape effectively the scattering patterns are mostly based on the engineering of the electric responses of various structures, such as optical Yagi–Uda antennas, V-shaped antennas, and bimetallic dimmers.[18,22–27] Recently, sub-wavelength high-index all-dielectric particles have also been used to manipulate the scattering direction[28,29] due to the resonance of their electric and magnetic modes and the low loss. Conventionally, the directional scattering is manipulated by carefully tuning the geometric parameters. However, this method is costly and, to certain extent, limited by the accuracy of fabrication process. Moreover, the dynamic control of the directional scattering is also highly desirable, which cannot be easily obtained in the geometry changing way.

Alternatively, the phase transition materials provide an effective way to control the far-field responses of nanostructures. Vanadium dioxide (VO_2), as a typical phase transition material, can be readily changed from semiconductor to metal state by controlling the ambient temperature.[30–34] This intriguing characteristic has been widely used to actively tune the plasmon response of metallic structure.[35,36] Dicken *et al.* reported a frequency-tunable metamaterial by deposing split-ring resonators on a VO_2 film in the mid-infrared region.[37] Ye and Drope investigated the plasmonic behavior of gold dimers tuned by a VO_2 nanoparticle in the gap.[38] Recently, thin VO_2 films have also been used to actively tune the beam steering angle of slot arrays[39] and switch the propagation direction of surface plasmon polariton (SPP) on metallic slabs.[40] Though a Yagi–Uda antenna for switchable radiation with VO_2 has been proposed,[41] the structure needs a rather complicated fabrication process. To the best of our knowledge,

*Project supported by the National Key R&D Program of China (Grant No. 2017YFA0303800), the National Natural Science Foundation of China (Grant Nos. 11634010, 61675170, and 11874050), the Natural Science Basic Research Plan in Shaanxi Province, China (Grant No. 2017JM6022), and the Fundamental Research Funds for the Central Universities, China (Grant No. 3102017zy017).

†Corresponding author. E-mail: fjxiao@nwpu.edu.cn

‡Corresponding author. E-mail: jlzhao@nwpu.edu.cn

© 2018 Chinese Physical Society and IOP Publishing Ltd

a simpler and readily fabricated structure with VO_2 for switchable directional scattering has not been reported yet. In this paper, we design an asymmetric Au–VO_2 nanodisk dimer for realizing switchable directional scattering. The directional scattering of the asymmetric dimer can be turned on/off by changing the VO_2 nanodisk from metal to semiconductor state. We envision that our results may pave a way in potential applications of compact thermo-optical sensors, directional surface plasmon resonance bio-sensing, and integrated nanophotonic systems.

2. Methods and model

The structure of the asymmetric Au–VO_2 nanodisk dimer is schematically shown in Fig. 1. This asymmetric dimer consists of two nanodisks of Au and VO_2 characterized by the following geometry parameters: height $T = 10$ nm, and diameters $D_{Au} = 100$ nm, $D_{VO_2} = 200$ nm. These two nanodisks with a surface-to-surface separation of 140 nm are placed in a vacuum ambient. The structure is under the excitation of a plane-wave with the propagation direction along the positive z axis and the polarization direction along the y axis. To study the scattering properties of the asymmetric dimer, we perform a full-wave simulation by the finite-difference time-domain (FDTD) method using commercial Lumerical Numerical Solutions. The permittivity of Au is obtained from empirically fitting the data of Johnson and Christy with the multi-coefficient model built in the software,[42] while the optical constants of VO_2 in metal and semiconductor states are taken from Ref. [43]. A perfectly matched layer (PML) boundary condition is used to mimic our structure in an infinitely large free space.

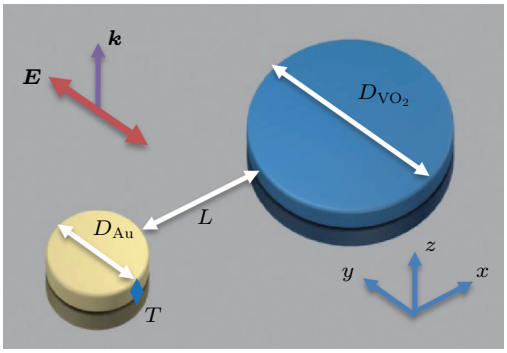


Fig. 1. (color online) Schematic view of an asymmetric dimer consisted of Au and VO_2 nanodisks. The incident plane-wave propagates in the positive z direction with the polarization along the y direction. The Au–VO_2 nanodisks with a separation gap $L = 140$ nm are positioned along the x axis. The sizes of these two disks are: thickness $T = 10$ nm, diameter $D_{Au} = 100$ nm for Au disk and $D_{VO_2} = 200$ nm for VO_2 disk.

The resonance wavelength of the dipole mode residing in the isolated Au (VO_2) nanodisk is determined from its scattering spectrum, as shown in Figs. 2(a) and 2(b). It can be seen that the peak around 700 nm (1500 nm) corresponds to the electric dipole mode of the Au nanodisk[44] (metallic VO_2 nanodisk[45]). This is further confirmed by the distributions of surface charge at the resonant wavelengths, as shown in Figs. 2(c) and 2(d). The scattering spectra of the VO_2 nanodisk indicate that LSPR exists in metallic VO_2 nanodisk at high temperature (355 K) but almost disappears in the semiconductor state at low temperature (300 K). It is attributed to the rise of intermediate states during the semiconductor-to-metal phase transition (SMT),[46,47] where these intermediate states can enhance the carrier density by increasing temperature. We investigate the far field scattering of the Au–VO_2 nanodisk dimer at the wavelength of 1.064 μm and examine the electromagnetic mode of VO_2 nanodisk at the semiconductor state. It is shown in Fig. 2(e) that, the VO_2 nanodisk at the wavelength of 1.064 μm gives purely electric dipole mode with a weaker charge confinement than that in metallic state.

We then employ a widely adopted two-dipole model[26,27,48] to describe the far-field scattering properties of the asymmetric dimer composed of Au (VO_2) nanodisks. To achieve directional scattering from the asymmetric dimer when the VO_2 nanodisk is in metallic state, we pay attention to the light scattered in the opposite directions along the line connecting the two particles, i.e., the opposite directions along the x axis in Fig. 1. The scattering intensity along this line is determined by $p_{Au}^2 + p_{VO_2}^2 + 2p_{Au}p_{VO_2}\cos(kl - \Delta\varphi)$, where $p_{Au(VO_2)}$ is the amplitude of the Au (VO_2) dipole, $k = \lambda/2\pi$ is the wave vector, l is the distance between the two dipoles, and $\Delta\varphi$ represents the intrinsic phase difference between them. The last term, describing the interference of the two dipoles, plays a significant role in achieving the directional scattering. Directional scattering would be obtained if interference is constructive in the positive x direction and destructive in the opposite direction. In the ideal case, the cosine function reaches the maximum value of perfect constructive interference ($kl - \Delta\varphi = 2\pi n$, n is an integer) when light propagates in the positive x direction, whereas it has the minimum value of perfect destructive interference ($-kl - \Delta\varphi = \pi + 2\pi n$) for light propagating in the negative x direction. This is equivalent to the condition of $l = \lambda/4$ and $\Delta\varphi = \pi/2$. The intrinsic phase difference $\Delta\varphi$ is determined by the complex particle polarizability, which can be calculated analytically with an approximation model in Ref. [27]. Figure 3(a) shows the scattering spectra of the asymmetric dimer with the VO_2 nanodisk in metallic and semiconductor states. A spectral peak of the Au nanodisk is prominent around 700 nm. The VO_2 nanodisk is a much weaker scatterer, so its dipole mode resonance ($\sim$ 1500 nm) is not easily discernible as a well-defined peak in the scattering spectra. The intrinsic phase differences between the two dipoles are shown in Fig. 3(b), where the red and blue curves correspond to VO_2 nanodisk in metallic and semiconductor states, respectively. It indicates that the intrinsic phase

difference $\Delta\varphi$ is close to $\pi/2$ between the two dipolar resonances of the asymmetric dimer when the VO_2 nanodisk is in metallic state, so the ideal case that interference of scattered light is perfect constructive in the positive x direction and perfect destructive in the opposite direction can be realized. Consequently, the directional scattering can be achieved in the wavelength range between dipolar resonances of the dimer with a precise tuning of the distance l, which corresponds to the dimer separation (center-to-center separation) of the two nanodisks. In order to achieve the directional scattering at a commercial laser wavelength of $\lambda = 1.064$ μm, the optimized $l = 290$ nm is adopted in our design. On the other hand, for the VO_2 nanodisk in semiconductor state, the ideal case of interference is no longer obtained and the directional scattering almost disappears. Thus, a switchable directional scattering can be achieved with the phase transition of the VO_2 nanodisk.

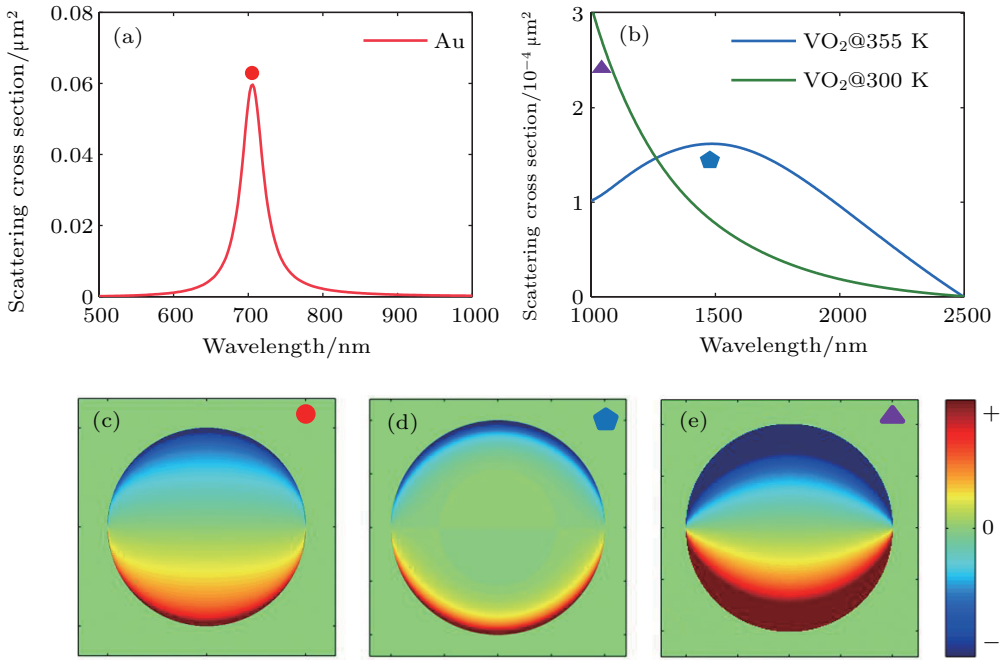


Fig. 2. (color online) (a) Scattering spectrum of individual Au nanodisk. (b) Scattering spectra of individual VO_2 nanodisk in the metallic (355 K) and semiconductor (300 K) states. (c) and (b) Calculated charge distributions at the resonant wavelength of Au (metallic VO_2) nanodisk indicated in (a) and (b), respectively. (e) Charge distribution of semiconducting VO_2 nanodisk excited at the wavelength of 1.064 μm.

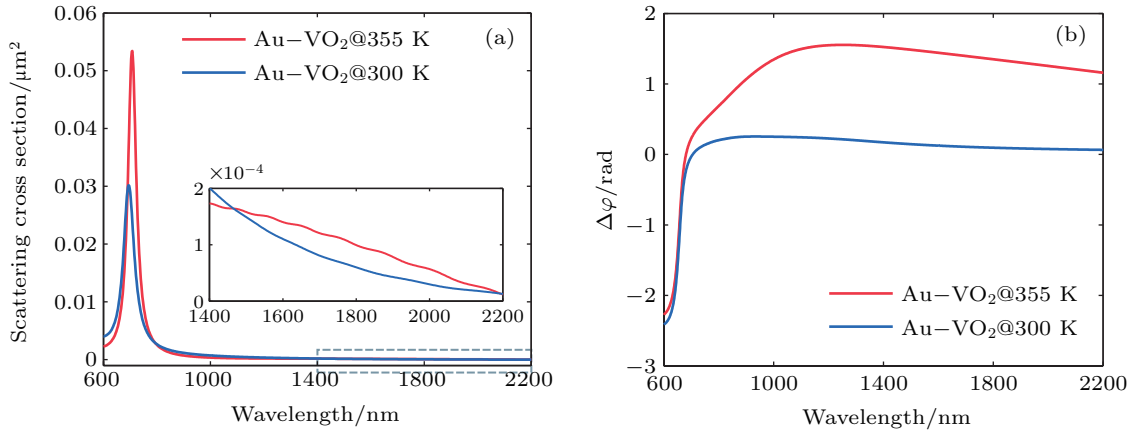


Fig. 3. (color online) (a) Scattering spectra of the asymmetric Au–VO_2 nanodisk dimer at 355 K (red curve) and 300 K (blue line). The inset is a magnified spectrum for the resonant peak corresponding to metallic VO_2 nanodisk. (b) Comparison of the relative phase difference between the dipoles in the asymmetric Au–VO_2 nanodisk dimer when VO_2 nanodisk is in metallic state (red curve) and semiconductor state (blue curve).

3. Result and discussion

Now we examine the electric field intensity distribution of the scattering light in the far-field at the excitation wavelength of 1.064 μm. Figures 4(a) and 4(b) display the normalized three-dimensional (3D) map of the far-field scattering intensity when the VO_2 nanodisk is in the metallic and semiconductor states, respectively. It shows a highly directional scattering in the positive x direction when the VO_2 nanodisk is in the metallic state at 355 K, and the directional scattering almost disappears when the VO_2 nanodisk changes to semi-

conductor state at 300 K. For a clear comparison, figures 4(c) and 4(d) show the normalized far-field scattering patterns of the asymmetric nanodisk dimer in polar coordinates of *xy* and *xz* planes when the VO_2 nanodisk is at different temperatures. To qualify the scattering directionality of the system, we introduce the directivity, i.e., a decibel comparison of scattering

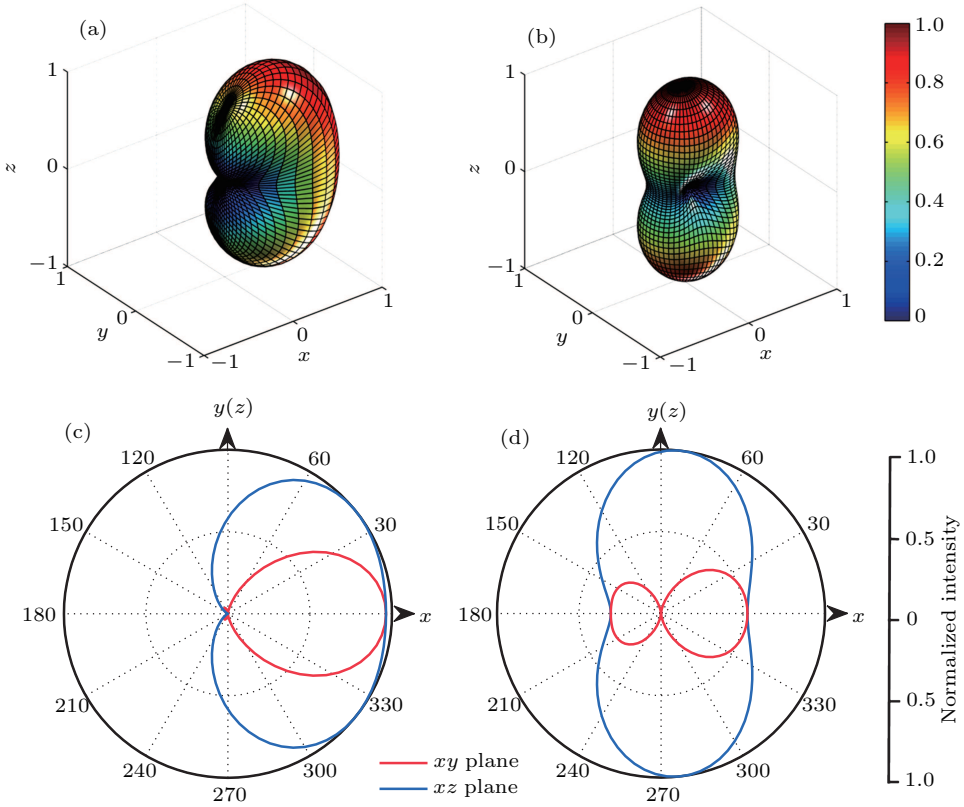


Fig. 4. (color online) (a), (b) Normalized 3D map of far-field scattering intensity for the asymmetric Au–VO_2 nanodisk dimer with the optimized dimer separation $l = 290$ nm excited by a plane-wave at $\lambda = 1.064$ μm at 355 K and 300 K. (c), (d) The corresponding scattering patterns ($|E|^2$) in *xy* (red curve) and *xz* (blue curve) planes at 355 K and 300 K.

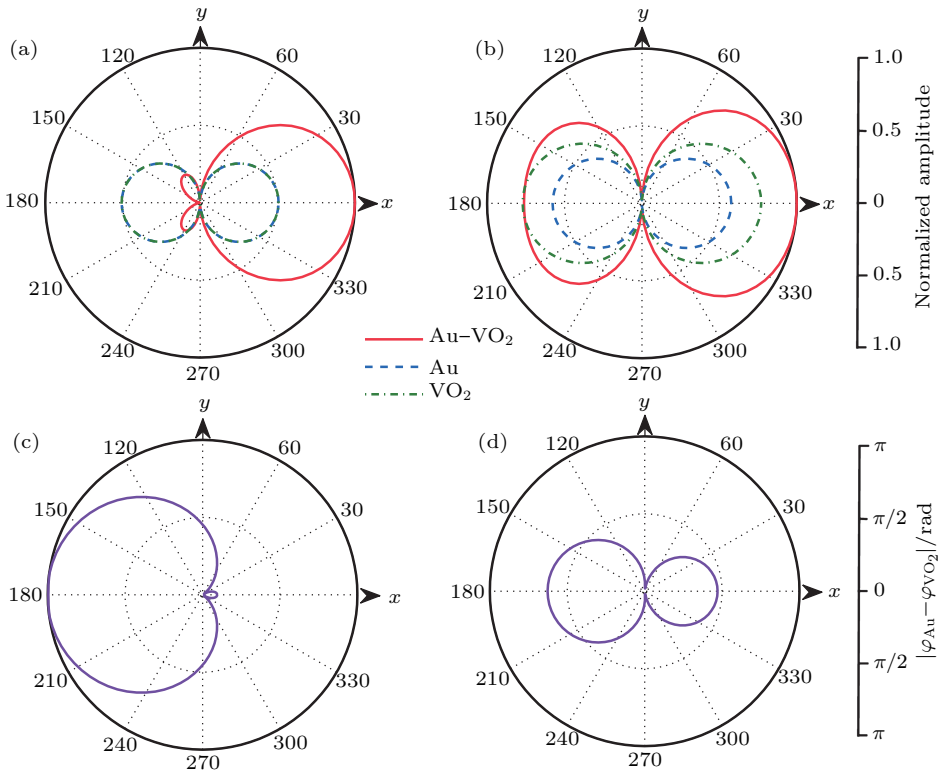


Fig. 5. (color online) (a), (b) Normalized far-field scattering amplitude patterns ($|E|$) of Au (blue dash curves), VO_2 (green dash curves) nanodisks, and asymmetric Au–VO_2 nanodisk dimer (red solid curves) in the *xy* plane under the excitation of 1.064 μm at 355 K and 300 K. (c), (d) Far-field phase difference $|\varphi_{Au} - \varphi_{VO_2}|$ between Au and metallic VO_2, semiconductor state VO_2 nanodisks, respectively.

intensity in the opposite direction $(10\log_{10}(I_{\rm p}/I_{\rm n}))$,[49,50] where $I_{\rm p(n)}$ is the scattering intensity in the positive (negative) x direction. It is found that the directivity can reach ~ 40 dB at 355 K, but it is only 2.3 dB at 300 K. This quantitative result indicates that a strongly directional scattering is achieved when the VO_2 nanodisk is in metallic state and it can be turned off with phase transition of the VO_2 nanodisk to the semiconductor state.

To explain the difference of the far-field scattering patterns for the two cases, we introduce an interference model and analyze the amplitudes of the scattered light from individual Au (VO_2) nanodisk and far-field phase difference between them. Figures 5(a) and 5(b) show the far-field scattering amplitudes of individual Au (VO_2) nanodisk and the asymmetric Au–VO_2 nanodisk dimer, all of which are normalized by the maximum amplitude of the asymmetric dimer under the corresponding temperature. The phase differences $|\varphi_{\rm Au} - \varphi_{\rm VO_2}|$ between the two nanodisks under different temperatures are shown in Figs. 5(c) and 5(d). The amplitudes of individual Au (VO_2) nanodisks are the same in the xy plane (Fig. 5(a)), and the phase difference between them is close to zero at the scattering angle of 0°, whereas it changes to π at the angle of 180° for the VO_2 nanodisk in metal state (Fig. 5(c)), leading to a perfectly directional scattering in the positive x direction. However, for the VO_2 nanodisk in semiconductor state, besides an obvious difference in amplitudes of the Au and VO_2 nanodisks (Fig. 5(b)), the phase differences between them are close to $\pi/2$ at two horizontal scattering angles as above (Fig. 5(d)), so the directional scattering cannot be achieved.

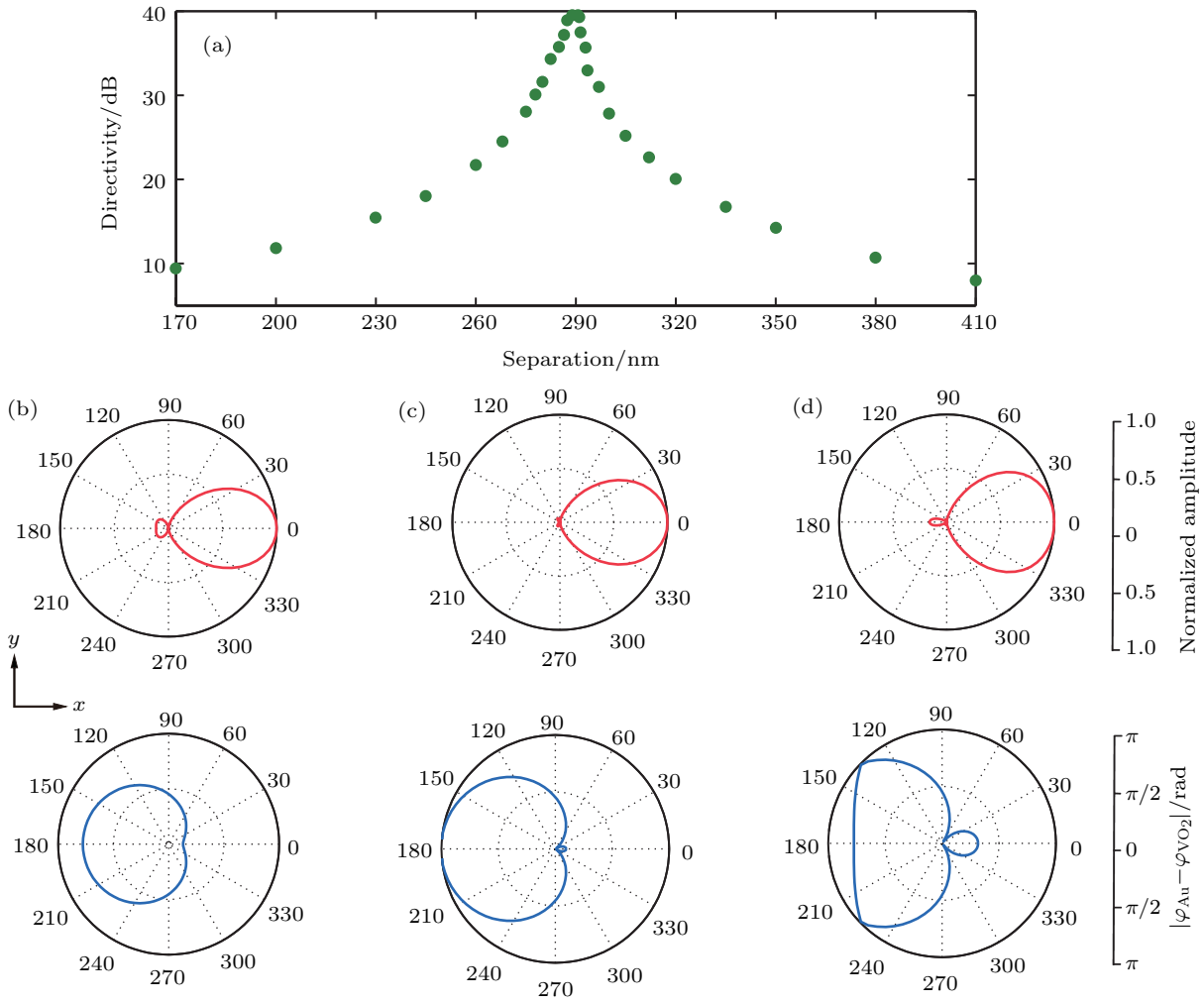


Fig. 6. (color online) (a) Dependence of directivity on dimer separation at ambient temperature of 355 K. (b)–(d) The normalized far-field scattering patterns ($|E|^2$) of the asymmetric Au–VO_2 nanodisk dimer (the upper panel) and corresponding phase differences $|\varphi_{\rm Au} - \varphi_{\rm VO_2}|$ between the two nanodisks (the lower panel) in xy planes with the dimer separations of $l = 170$ nm, $l = 290$ nm, and $l = 410$ nm, repsectively.

In the following, we investigate the dependence of the directivity on the dimer separation. The results are displayed in Fig. 6. It is found that the directivity decreases when the dimer separation deviates away from the optimized separation of 290 nm as shown in Fig. 6(a). This can be further examined by three representative scattering patterns with dimer separations of 170 nm, 290 nm, and 410 nm, as shown in the upper panel of Figs. 6(b)–6(d). The corresponding directivities are 9.4 dB, 39.6 dB, and 8.0 dB for the dimer separations of 170 nm, 290 nm, and 410 nm, respectively. To unravel

the directivity change in Figs. 6(b)–6(d), we depict the polar plot of their phase differences $|\varphi_{Au} - \varphi_{VO_2}|$ in the lower panel of Figs. 6(b)–6(d). It is found that the phase differences $|\varphi_{Au} - \varphi_{VO_2}|$ along the negative x direction are 0.78π, π, and 0.77π when the separation is increased from 170 nm to 290 nm and 410 nm. As a result, a nearly perfect destructive interference along the negative x direction (a high underlying directivity) is observed for the dimer separation of 290 nm. However, the partially destructive interference occurs as the dimer separation is deviated from 290 nm, resulting in a decreased directivity shown in Figs. 6(b) and 6(d). It is worth noting that the directivity change in Fig. 6(a) is as large as 32 dB, which achieves almost the same quantity to that mediated by the phase transition of VO_2 (37 dB). However, the phase transition controlled directivity can avoid the rather complex fabrication process of separation change, enjoying more flexibility.

4. Conclusion

In summary, we have designed an asymmetric Au–VO_2 nanodisk dimer for switchable directional scattering. The two peaks, determined from the scattering spectrum, correspond to the electronic dipole modes of Au (metal VO_2) nanodisk, and the modes are confirmed by the distributions of surface charge. The phase difference between the two dipoles is large enough for satisfying the ideal case of interference for the scattered light propagating to the opposite directions along the line connecting these two nanodisks, which results in a strongly directional scattering with the directivity of ~ 40 dB towards to the metallic VO_2 nanodisk. However, the directional scattering almost disappears (2.3 dB) when the VO_2 nanodisk changes to semiconductor state. We further propose an effective method to switch the directional scattering on/off based on the SMT of VO_2 nanodisk. This tunable directional scattering is well interpreted from far-field phase difference between the two nanodisks with an interference model. Our result may have potential applications in compact thermo-optical sensors, directional surface plasmon resonance bio-sensing, and integrated nanophotonic systems.

References

[1] Gramotnev D K and Bozhevolni S I 2010 *Nat. Photon.* **4** 83
[2] Svedendahl M, Chen S, Dmitriev A and Käll M 2009 *Nano Lett.* **9** 4428
[3] Park J, Estrada A, Sharp K, Sang K, Schwartz J A, Smith D K, Coleman C, Payne J D, Korgel B A, Dunn A K and Tunnell J W 2008 *Opt. Express* **16** 1590
[4] Howes P D, Rana S and Stevens M M 2014 *Chem. Soc. Rev.* **43** 3835
[5] Li K R, Stockman M I and Bergman D J 2003 *Phys. Rev. Lett.* **91** 227402
[6] Shang W Y, Xiao F J, Zhu W R, He H S, Premaratne M, Mei T and Zhao J L 2017 *Sci. Rep.* **7** 1049
[7] Xiao F J, Zhu W R, Shang W Y, Mei T, Premaratne M and Zhao J L 2015 *Opt. Express* **23** 3236
[8] Shang W Y, Xiao F J, Han L, Premaratne M, Mei T and Zhao J L 2018 *J. Phys.: Condens. Matter* **30** 064004
[9] Celebrano M, Wu X F, Baselli M, Großmann S, Biagioni P, Locatelli A, Angelis D C, Cerullo G, Osellame R, Hecht B, Duò L, Ciccacci F and Finazzi M 2015 *Nat. Nanotech.* **10** 412
[10] Xiao F J, Shang W Y, Zhu W R, Han L, Premaratne M, Mei T and Zhao J L 2018 *Photon. Res.* **6** 157
[11] Pompa P P, Martiradonna L, Torre A D, Sala F D, Manna L, De Vittorio M, Calabi F, Cingolani R and Rinaldi R 2006 *Nat. Nanotech.* **1** 126
[12] Aioub M and El-Sayed M A 2016 *J. Am. Chem. Soc.* **138** 1258
[13] Prodan E and Nordlander P 2004 *J. Chem. Phys.* **120** 5444
[14] Kim S, Jin J, Kim Y J, Park I Y, Kim Y and Kim S W 2008 *Nature* **453** 757
[15] Yang L K, Wang H C, Fang Y and Li Z P 2016 *ACS Nano* **10** 1580
[16] Lassiter J B, Sobhani H, Fan J A, Kundu J, Capasso F, Nordlander P and Halas N J 2010 *Nano Lett.* **10** 3184
[17] Xiao F J, Zhu W R, Premaratne M and Zhao J L 2014 *Opt. Express* **22** 2132
[18] Curto A G, Volpe G, Taminiau T H, Kreuzer M P, Quidant R and van Hulst N F 2010 *Science* **329** 930
[19] Valuckas V, Paniagua-Dominguez R, Fu Y H, Luk'yanchuk B and Kuznetsov A I 2017 *Appl. Phys. Lett.* **110** 091108
[20] Evlyukhin A B, Bozhevolnyi S I, Pors A, Nielsen M G, Radko I P, Willatzen M and Albrektsen O 2010 *Nano Lett.* **10** 4571
[21] Atwater H A and Polman A 2010 *Nat. Mater.* **9** 205
[22] Ding W, Chen Y H and Li Z Y 2014 *Chin. Phys. B* **23** 037301
[23] Tribelsky M I, Geffrin J M, Litman A, Eyraud C and Moreno F 2016 *Phys. Rev. B* **94** 121110
[24] Coenen T, Vesssur E J, Polman A, Koenderink A F 2011 *Nano Lett.* **11** 3779
[25] Hu D J, Zhang Z Y and Du J L 2015 *Chin. Phys. B* **24** 104202
[26] Vercruysse D, Sonnefraud Y, Verellen N, Fuchs F B, Di Martino G, Lagae L, Moshchalkov V V, Maier S A, Van Dorpe P 2013 *Nano Lett.* **13** 3843
[27] Shegai T, Chen S, Miljkovic V D, Zengin G, Johansson P and Käll M 2011 *Nat. Commun.* **2** 481
[28] Liu W, Zhang J F, Lei B, Ma H T, Xie W K and Hu H J 2014 *Opt. Express* **22** 16178
[29] Tian J Y, Li Q, Yang Y Q and Qiu M 2016 *Nanoscale* **8** 4047
[30] Cavalleri A, Tóth C, Siders C W, Squier J A, Ráksi F, Forget P and Kieffer J C 2001 *Phys. Rev. Lett.* **87** 237401
[31] Abb M, Albella P, Aizpurua J and Muskens O L 2011 *Nano Lett.* **11** 2457
[32] Kats M A, Blanchard R, Genevet P, Yang Z, Qazilbash M M, Basov D, Ramanathan S and Capasso F 2013 *Opt. Lett.* **38** 368
[33] Paik T, Hong S H, Gaulding E A, Caglayan H, Gordon T R, Engheta N, Kagan C R and Murray C B 2014 *ACS Nano* **8** 797
[34] Michel A K U, Zalden P, Chigrin D N, Wuttig M, Lindenberg A M and Taubner T 2014 *ACS Photon.* **1** 833
[35] Zhou H J, Cao X, Jiang M, Bao S H and Jin P 2014 *Laser Photon. Rev.* **8** 617
[36] Liu H W, Lu J P and Wang X R 2018 *Nanotechnology* **29** 024002
[37] Dicken M J, Aydin K, Pryce I M, Sweatlock L A, Boyd E M, Walavalkar S, Ma J and Atwater H A 2009 *Opt. Express* **17** 18330
[38] Ye J and Dorpea P V 2012 *Nanoscale* **4** 7205
[39] Kaplan G, Aydin K and Scheuer J 2015 *Opt. Mater. Express* **5** 2513
[40] Kim S J, Yun H, Park K, Hong J, Yun J G, Lee K, Kim J, Jeong S J, Mun S E, Sung J, Lee Y W and Lee B 2017 *Sci. Rep.* **7** 43723
[41] Rahimi E and Sendur K 2017 *Opt. Commun.* **392** 109
[42] Johnson P B and Christy R W 1972 *Phys. Rev. B* **6** 4370
[43] Verleur H W, Barker A S and Berglund C N 1968 *Phys. Rev.* **172** 788
[44] Khan Y, Li A R, Chang L, Li L D and Guo L 2018 *Sensors Actuat. B-Chem.* **255** 1298
[45] Lopez R, Haynes T E, Boatner L A, Feldman L C and Haglund R F 2002 *Opt. Lett.* **27** 1327
[46] Kumar S, Strachan J P, Pickett M D, Bratkovsky A, Nishi Y and Williams R S 2014 *Adv. Mater.* **26** 7505
[47] Ke Y J, Wen X L, Zhao D Y, Che R C, Xiong Q H and Long Y 2017 *ACS Nano* **11** 7542
[48] Lu G W, Wang Y W, Chou R Y, Shen H M, He Y B, Cheng Y Q and Gong Q H 2015 *Laser Photon. Rev.* **9** 530
[49] Pakizeh T and Käll M 2009 *Nano Lett.* **9** 2343
[50] Shegai T, Miljković V D, Bao K, Xu H X, Nordlander P, Johansson P and Käll M 2011 *Nano Lett.* **11** 706